# Properties of Magnetic Neutral Line Gradients and Formation of Filaments

**Nina V. Karachik · Alexei A. Pevtsov**

**Abstract** We investigate the gradients of magnetic fields across neutral lines (NLs) and compare their properties for NLs with and without chromospheric filaments. Our results show that there is a range of preferred magnetic field gradients where the filament formation is enhanced. On the other hand, a horizontal gradient of the magnetic field across an NL alone does not appear to be a single factor that determines if a filament will form (or not) in a given location.

## 1. Introduction

Chromospheric filaments (prominences at the limb) are one of the major features characterizing solar activity in the low solar atmosphere (the chromosphere and low corona). Filament eruptions are at the core of many solar-terrestrial (space weather) effects. The filaments are formed along magnetic polarity inversion lines, but only a minority of these neutral lines (NLs) have filaments above them. Several studies have attempted to find the necessary conditions for filament formation, but we still lack a clear understanding of this phenomenon (Mackay *et al.*, 2010). Previous studies found that filaments form only in filament channels (for a review, see Gaizauskas, 1998) which overlay NLs. Some studies have indicated that the convergence of magnetic flux leading to flux cancellation (reconnection) is required for filament formation (see Mackay, Gaizauskas, and Yeates, 2008; Martin, 1990, 1998; and references therein). Recently, Martin *et al.* (2012) suggested that formation of filaments and filament channels is part of the development of large-scale chiral systems. In our present study, we concentrate only on properties of NLs and do not consider other aspects of filament formation (for example, the role of helicity).

N.V. Karachik · A.A. Pevtsov (✉)
National Solar Observatory, Sunspot, NM 88349, USA
e-mail: apevtsov@nso.edu

N.V. Karachik
e-mail: nkarachi@nso.edu

Gaizauskas, Mackay, and Harvey (2001) have shown that one important condition for the formation of a filament channel is a strong horizontal component of a magnetic field aligned with the magnetic NL. Thus, one may ask: Are the properties (and evolution) of magnetic NLs sufficient to identify the potential location of filament formation? Indeed, several studies (*e.g.*, Maksimov and Prokopiev, 1995; Nagabhushana and Gokhale, 1990) have suggested that the gradient of the magnetic field transverse to the neutral line may play a significant role in filament formation. According to Démoulin (1998), one of the necessary conditions for filament formation is a low gradient of the magnetic field transverse to the NL.

Here we conduct a statistical study of horizontal gradients of magnetic fields across NLs and investigate how these properties differ for NLs with filaments and without them. We also investigate whether the properties of NLs change with the solar cycle and, if so, whether this change can be the cause of variation in the length and total number of filaments with the solar cycle.

## 2. Data and Data Analysis

We employ daily Hα full-disk images from the Mauna Loa Solar Observatory (MLSO) and *Solar and Heliospheric Observatory* (SOHO)/*Michelson Doppler Imager* (MDI) synoptic maps for the years 1997 – 2010. For our main Hα data set, we included daily full-disk images corresponding to two complete Carrington rotations (CRs) per year with a time separation between selected CRs of about five months. However, due to a lack of data, only one rotation was taken for the years 1997, 2003, and 2010; for the year 2000, we selected three (nonconsecutive) solar rotations. In addition to MDI synoptic maps (for the same CRs as our Hα data), we also use *Synoptic Optical Long-term Investigations of the Sun* (SOLIS, Balasubramaniam and Pevtsov, 2011) synoptic maps and full-disk magnetograms taken at the Ca II 854.2 nm chromospheric line to study properties of the chromospheric NLs.

Because of the statistical nature of our study, we automated the identification of filaments (using Hα full-disk images) and NLs (using MDI synoptic maps). Several studies were made to develop filament automatic detection (*e.g.*, Shih and Kowalski, 2003; Qu *et al.*, 2005; Scholl and Habbal, 2008; Joshi, Srivastava, and Mathew, 2010). Most of them have an extensive algorithm of filament detection from an image taken in a single wavelength or use multiple images taken in different wavelengths. In our algorithm, we used both Hα daily full-disk images and magnetograms. This allowed us to significantly simplify the process of filament detection by comparing the location of potential filaments (dark features initially found on Hα images) with the underlying magnetic field. This approach also helped to reduce the (computer) processing time.

The criterion for filament identification is an intensity threshold which is defined as an average intensity over the full-disk image minus two standard deviations of the average. All pixels satisfying this criterion (but excluding pixels near the limb) are considered as potential filaments. The final selection takes into account the existence of an NL inside the filament contour. Magnetic NLs were identified on synoptic maps after smoothing them with a $50 \times 50$ pixel running window.

Figure 1 shows an example of an Hα full-disk image with filament contours found by our automated procedure. Clearly, our procedure successfully identifies all major filaments, although small clumps of filament material could be missed, especially in locations near the solar limb. For example, while the procedure identifies one clump of filament material near the north polar region (near the top of the solar disk in Figure 1), it misses several other

**Figure 1** Hα full-disk image (taken on 9 January 2000 at 18:44:19 UT) with filament contours as identified by our automated procedure.
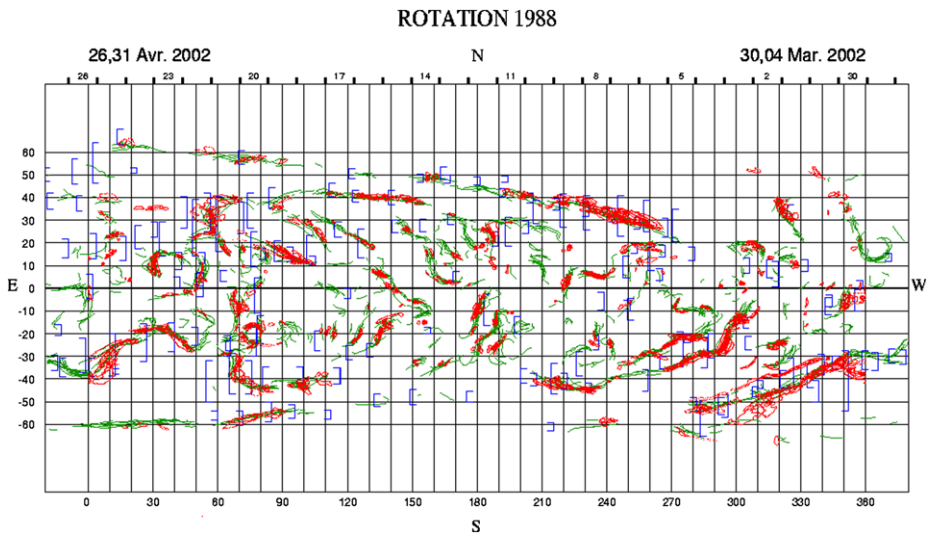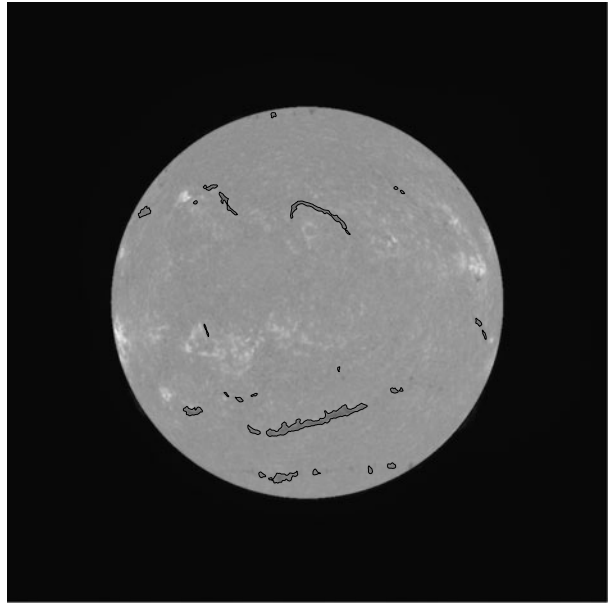




**Figure 2** Filaments from BASS2000 Solar Survey database (green) and our identification method (red).

clumps in the same location. As an additional test, for a few selected solar rotations, we compared our filament identification with the data from the BASS2000 Solar Survey database (bass2000.obspm.fr). Figure 2 demonstrates a very good agreement between filaments from the BASS2000 database (green) and those identified by our method (red).

Figure 3 is an MDI synoptic map with NLs drawn in different colors. The colors are used to indicate the type of NL: green for the lines between magnetic polarities inside one active region, and red for the lines separating polarities of two different active regions. For reasons
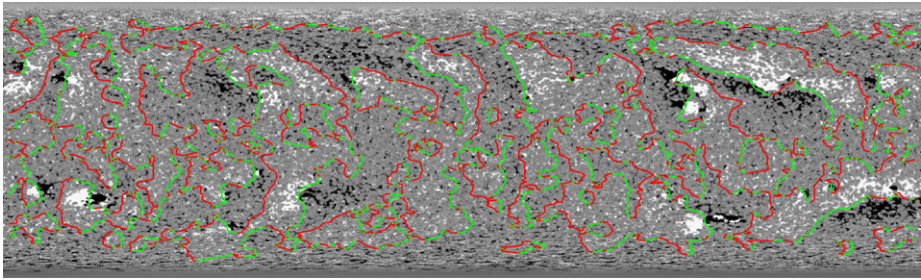
**Figure 3** Example of MDI synoptic map for Carrington rotation 1932 with NLs. Green color is used for type A lines (inside one bipolar region), and red is for type B lines (between two bipolar regions). Black/white corresponds to negative/positive polarities.
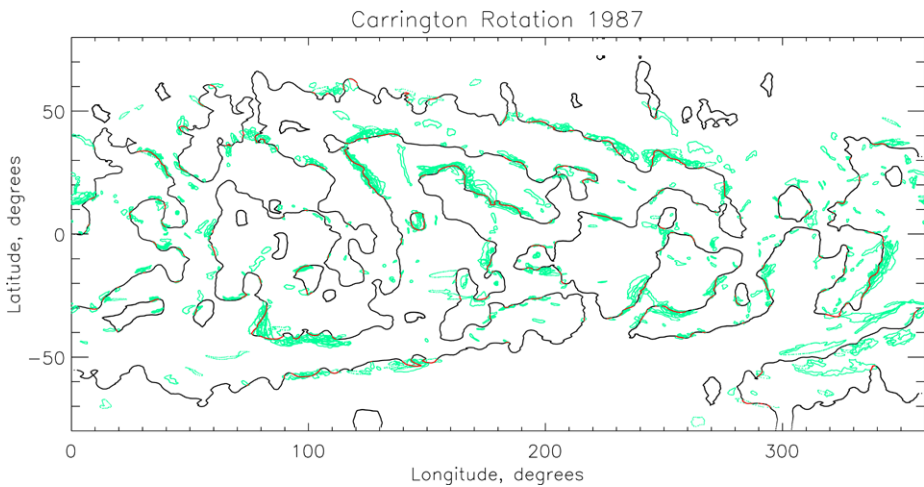


**Figure 4** Example of NLs (black) with filament contours (green). Parts of NLs that have filaments are indicated in red.

of automation, the determination of a type of NL (inter-/intra-active region) is based on the polarity of fields to the West and East of the NL. If the orientation of these two polarities followed the Hale polarity rule, we called the line an intra-active region NL; otherwise, it was classified as an inter-region NL. Inevitably, this approach misidentifies non-Hale polarity active regions. But the fraction of such regions is very minor, and thus the effect on the overall statistics is insignificant.

Figure 4 provides an example of NLs associated with the chromospheric filaments as identified by our procedure. The portions of NLs with filaments are marked in red.

Although we analyze only two solar rotations per year, our data set of filaments is representative of complete data. For example, the latitudinal distribution of filaments in our data set exhibits the well-known latitudinal drift (see, *e.g.*, Li, 2010). During the rising phase of solar activity, the filament distribution (in our set) shows a clear preference for high latitudes, and as the cycle progresses, more filaments are found at lower latitudes following the equatorward drift, similar to the sunspot butterfly diagram.
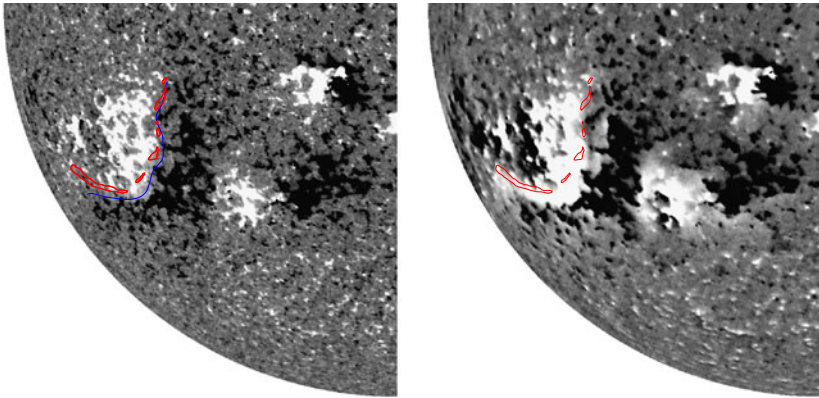
**Figure 5** Example of filament displacement with respect to the NL on photospheric (left) and chromospheric (right) magnetograms from VSM on SOLIS. Blue line represents the NL, red contour the location of a filament. Black/white corresponds to negative/positive polarities.

## 3. Displacement of Filaments with Respect to Neutral Lines

While the chromospheric filaments are located above the magnetic NLs, it is not uncommon to see a displacement between the location of an NL (as measured in the photosphere) and the filament body (as observed in Hα) in the full-disk images. One can contribute this displacement to the fact that filaments are features located at certain heights above the photosphere and to their projection to the image plane.

However, our analysis suggests that this displacement cannot be explained by a simple projection effect alone. To further explore this displacement, we analyzed a number of filaments observed near the central meridian. High-latitude filaments ($|lat| \geq 60$ degrees) were excluded from this analysis. We also compared the change in filament-NL displacements for selected filaments near the East and West limbs. The displacements between the filament body and the NL were present in different locations independent of closeness to the limb or the central meridian. In some cases, only a part of a filament was displaced relative to the closest NL, while the rest of the filament was perfectly aligned with the NL. Figure 5 (left panel) shows one such example.

Since the filaments could be located at a certain height above the photosphere, one could argue that their location should correlate better with the NLs of the chromospheric fields (which are formed higher in the atmosphere). Contrary to this expectation, some filaments show a larger displacement relative to the closest chromospheric NL as compared with the photospheric NL (compare the left and right panels in Figure 5). Thus, the displacement of filament location (as shown in the image plane of the photospheric and chromospheric magnetograms) is clearly not due to a projection effect alone.

One possible explanation for these displacements is that the "neutral lines" are not lines but planes separating opposite polarities. These "polarity inversion planes" are not always vertical, but can be inclined depending on the flux systems they separate. One can visualize this as a ribbon (perhaps, a current sheet) "waving" around the isolated coronal flux systems. The intersection of this polarity inversion plane with the photosphere corresponds to the photospheric NL, and the filament can form higher up within this plane. If this interpretation is correct, the displacement between the photospheric NL and filament body would be an interplay between the location (height) of the filament within the polarity inversion
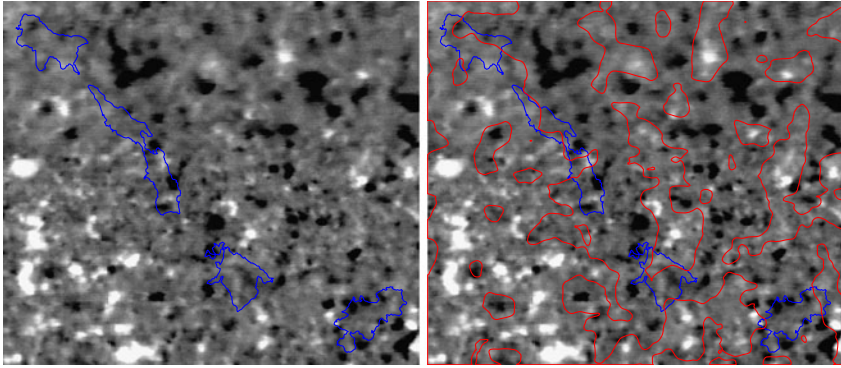
**Figure 6** Example of a filament contour (blue) displayed on magnetogram. Red color is used for NLs. Black/white corresponds to negative/positive polarities.

plane and the tilt of the plane relative to the solar surface. The idea that (some) chromospheric filaments are sheet-like structures is not new. We simply use it to demonstrate that the broadly held belief that the filaments are located above magnetic NLs should be taken with a clear understanding that in the image plane the location of filament bodies and NLs could be displaced from each other, not only due to the elevation of a filament above the photosphere, but also because of its height geometry.

In some cases of relatively weak (and fragmented) magnetic fields, the exact location of the photospheric NL is very uncertain. In some of these cases, a continuous photospheric NL may not even exist underneath a filament. For example, the filament segment in the lower right corner of Figure 6 overlies a patch of negative polarity; no clear NL (of the photospheric field) appears to be associated with this filament segment.

The inconsistencies between the location of filaments and the photospheric/chromospheric NLs described in this section may indicate that the filament location is governed by the coronal magnetic fields rather than the photospheric or even the chromospheric fields.

As a rule, we find a better agreement between the neutral lines and filament positions when we use synoptic maps. We speculate that since these maps are based on an averaged magnetic field, they may better represent the large-scale magnetic domains. Even though for filament identification we employ daily full-disk images, we do average the filament positions over several days in order to minimize any projection effects. Based on the results of the analysis presented in this section, for our study of magnetic properties of NLs we chose to use the synoptic magnetograms.

## 4. Role of Gradient of Magnetic Field

First, we investigate gradients of the magnetic field across the NL and their variation with the level of solar activity. Figure 7 shows the temporal variation of the gradient distribution for NLs with filaments (left panel) and without them (right panel). The gradients were computed at uniformly spaced intervals along the magnetic NLs. Then, each segment was identified as either having a filament or not based on the proximity of filament material to this part of the NL. We did not attempt any averaging of field gradients for individual filaments. Different colors are used to indicate the fraction of NLs with a specific property; for example, the contour labeled 0.95 means that 95 % of the NLs have gradients less than or equal to the
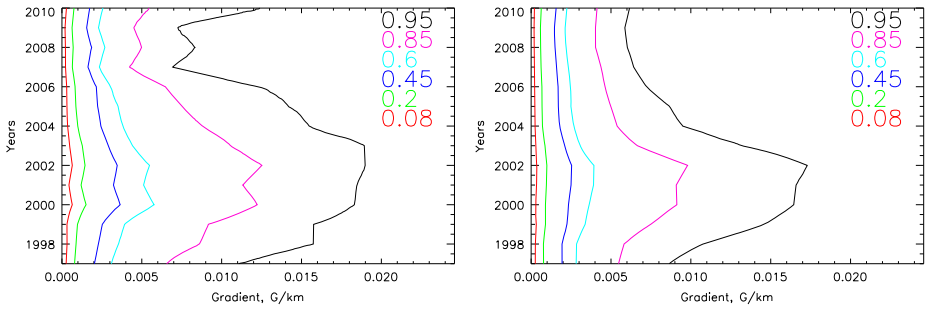
**Figure 7** Temporal variation of gradient distribution. Left: NLs with filaments, right: lines without filaments. Colored contours correspond to fraction of gradients below a certain value. For instance, for the year 1997 95 % of all NLs without filaments have gradients below 0.0088 G km$^{-1}$ (right panel).

gradient shown as the abscissa on Figure 7. As an example, for the year 1997, 95 % of NLs with filaments (Figure 7, left) have gradients $\leq 0.011$ G km$^{-1}$, while 95 % of NLs without filaments (Figure 7, right) have gradients $\leq 0.0088$ G km$^{-1}$.

At first glance, the distributions of gradients across NLs with and without filaments are very similar. However, NLs with filaments exhibit systematically stronger gradients compared to NLs without filaments (compare Figure 7, left and right panels). Filaments are observed above the NLs with gradients ranging from $6.6 \times 10^{-5}$ G km$^{-1}$ to 0.11 G km$^{-1}$. Only a small fraction of filaments are formed above the NLs with gradients outside that range. The fraction of NLs with gradients smaller than about 0.001 G km$^{-1}$ is about 20 % for NLs with or without filaments, and it does not seem to vary with solar activity cycle. The fraction of NLs with gradients higher than 0.005 G km$^{-1}$ shows a strong variation with solar activity cycle. By its amplitude, NLs with and without filaments show a comparable change between solar minimum and maximum: for NLs with filaments, the 95 % level decreases from about 0.019 G km$^{-1}$ (year 2002) to about 0.007 G km$^{-1}$ (year 2009), while for NLs without filaments it changes from 0.017 G km$^{-1}$ (year 2002) to 0.006 G km$^{-1}$ (year 2009). However, the changes for NLs with filaments occur over a longer period of time (*i.e.*, the peak corresponding to the 95 % level in the left panel of Figure 7 is much "broader" compared with that in the right panel of Figure 7). In 2002, about 50 % (between the 0.95 and 0.45 contours in Figure 7) of NLs with filaments fall within $0.019 - 0.0035$ G km$^{-1}$. In the same year, 35 % of all filaments (between the 0.95 and 0.45 contours in Figure 7) formed above NLs within a $0.019 - 0.005$ G km$^{-1}$ range of gradients. In comparison, 50 % of NLs without filaments fell within $0.017 - 0.0025$ G km$^{-1}$, and 35 % of NLs (without filaments) were in the $0.017 - 0.004$ G km$^{-1}$ range. In 2004, 50 % of filaments (the $0.95 - 0.45$ levels in Figure 7) developed above NLs with $0.0155 - 0.0022$ G km$^{-1}$ magnetic field gradients, while 50 % of NLs without filaments fell within the $0.0095 - 0.0018$ G km$^{-1}$ range of gradients. During periods of low sunspot activity (*i.e.*, $2007 - 2009$), NLs with and without filaments had a similar range of gradients (*e.g.*, in 2007, 85 % of NLs with and without filaments were below about 0.005 G km$^{-1}$; compare Figure 7, left and right panels).

Thus, our data show a clear tendency for NLs with filaments to have stronger magnetic gradients during the rising and declining phases and the solar cycle maximum, compared to NLs without filaments. Although filaments are formed above the NLs with a wide range of gradients, there appears to be a preferred range of gradients where filaments are observed more often. This preferred range covers gradients from about 0.0025 to 0.019 G km$^{-1}$. Less than 20 % of filaments were formed at gradients below about 0.001 G km$^{-1}$, and less than
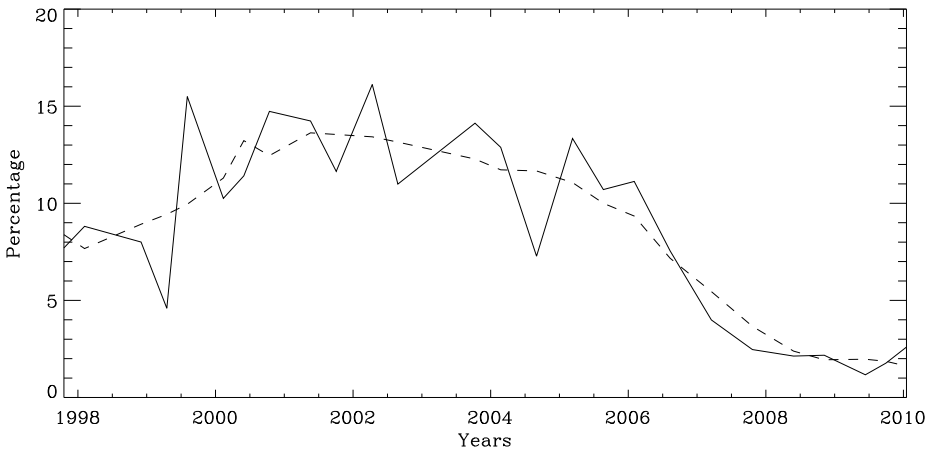
**Figure 8** Fraction of NL total length occupied by filaments as a function of time. Solid line shows measurements from selected Carrington rotations, and the dashed line represents five-point central moving average.

about 5 % of filaments have developed above NLs with 0.0019 G km$^{-1}$ (at solar maximum). On the other hand, having a "preferred" horizontal gradient does not guarantee filament formation there; a large fraction of NLs which exhibit similar gradients remain empty of filament material. Furthermore, on average, only a small fraction of NLs are associated with filaments. This fraction varies from about 2 % at solar minimum to 15 % at solar maximum (Figure 8).

Next, we investigate the properties of magnetic field gradients for different types of filament. One of the earliest classification schemes (see, *e.g.*, Tang, 1987) segregates filaments into two categories based on the nature of the NL above which the filament lies. If a filament overlays an NL separating two polarities forming an active region, it is classified as a "bipolar region filament" (type A). When a filament is formed above an NL that separates two different active regions, it is called a "between bipolar region filament" (type B). To automate the categorization of NLs, we assigned their type based on magnetic polarity orientation and the Hale polarity rule (*i.e.*, if the (leading-following) polarity orientation for a given NL agreed with the Hale–Nicholson polarity rule, this NL and filament above it were classified as type A). Otherwise, the NL (and the filament) were classified as type B. An example of this classification is shown in Figure 3. The color green is used to indicate type A lines, and red is used for type B. Although this simplified approach allows an automatic identification of the type of NLs and filaments, it has the limitation of misidentifying NLs and filaments associated with non-Hale polarity regions. Likely, only a small fraction (about a few percent) of all active regions disobey the Hale–Nicholson polarity rule.

Two types of NLs (and filaments) do not appear to show any significant difference in properties of magnetic gradients. However, we did find a slight tendency for filaments to form in between active regions (type B) at a rising phase of the solar cycle, while type A filaments (inside active region) were more abundant at the declining phase of the cycle.

Lastly, we expanded our investigation to the NLs derived from the chromospheric magnetic fields observed by the *Vector Spectromagnetograph* (VSM) on SOLIS. We applied the same technique as for the photospheric magnetograms. The results are very similar to those derived from the photospheric fields with respect to the pattern of gradients described above.

## 5. Discussion

We studied the properties of horizontal gradients across neutral lines (NLs) depending on the presence or absence of filaments above them. We found a preferred range of NL gradients where filaments are observed relatively more frequently. Still only about 18 % of NLs within that "preferred range" of gradients have filaments above them. Thus, the mere fact that a horizontal gradient across a magnetic NL falls within a "preferred" range does not guarantee that a filament will form in that location. However, one cannot exclude that, together with other factors, these gradient properties could play a role in creating overall conditions for filament formation. Several studies suggested that magnetic field convergence may be required for filament formation (*e.g.*, Martin, 1990, 1998; Mackay, Gaizauskas, and Yeates, 2008). Another factor that could play an important role in filament formation is the rate of canceling magnetic features that were hypothesized to supply the material to filaments (Martin, 1998; Litvinenko and Martin, 1999). Due to spatial and temporal limitations of the data set used in this study, we did not investigate the roles of these other factors in filament formation.

The gradients for NLs with filaments show similar variations with the solar cycle as those for the NLs without filaments (*i.e.*, an increase in the fraction of stronger gradients during the maximum of solar activity). However, this change in properties of gradients for NLs with filaments is enhanced during the rising and declining phases of the cycle, while the properties of NLs without filaments are more narrowly defined to the maximum of the solar cycle. During these periods (of rising and declining phases of the solar cycle), a larger fraction of the NLs within the preferred range of gradients are occupied by filaments.

Although we did not find a strong preponderance of filament formation depending on the properties of magnetic gradients of NLs, our data do suggest that there is a range of magnetic gradients preferred for filament formation. A cyclic increase in the fraction of NLs (with these preferred gradients) may enhance favorable conditions for more filament formation during a solar maximum. However, an additional mechanism(s) that takes advantage of the above favorable conditions to create more filaments is needed. This additional condition could be the amount of material in the corona available for filament formation. One can speculate that during solar maximum, overall conditions in the photosphere and chromosphere (enhanced network fields, larger number of small-scale reconnection events, *etc.*) may result in a significantly larger amount of material supplied to the corona. In combination with the increased fraction of NLs with stronger gradients, the presence of more material in the corona may create more opportunities for condensation of this material to form the chromospheric filaments.

Finally, the noted displacement of filaments (with respect to the photospheric NLs) and the lack of a strong correlation between the gradient properties of NLs and filament formation may suggest that filament formation is governed by properties of coronal magnetic fields rather than the photospheric or chromospheric magnetic fields. In itself, this may fit better with a model in which the excess of material in the corona combined with changes in properties of NLs at solar cycle maximum is the prime reason for a solar cycle variation in chromospheric filaments. At present, no such model exists.

## References

Balasubramaniam, K.S., Pevtsov, A.: 2011, In: *Proc. SPIE* **8148**, SPIE, Bellingham, 814809.
Démoulin, P.: 1998, In: Webb, D., Rust, D., Schmieder, B. (eds.) *IAU Colloq. 167: New Perspectives on Solar Prominences*, *ASP Conf. Series* **150**, ASP, San Francisco, 78.
Gaizauskas, V.: 1998, In: Webb, D., Rust, D., Schmieder, B. (eds.) *IAU Colloq. 167: New Perspectives on Solar Prominences*, *ASP Conf. Series* **150**, ASP, San Francisco, 257.
Gaizauskas, V., Mackay, D.H., Harvey, K.L.: 2001, *Astrophys. J.* **558**, 888.
Joshi, A.D., Srivastava, N., Mathew, S.K.: 2010, *Solar Phys.* **262**, 425.
Li, K.J.: 2010, *Mon. Not. Roy. Astron. Soc.* **405**, 1040.
Litvinenko, Y.E., Martin, S.F.: 1999, *Solar Phys.* **190**, 45.
Mackay, D.H., Gaizauskas, V., Yeates, A.R.: 2008, *Solar Phys.* **248**, 51.
Mackay, D.H., Karpen, J.T., Ballester, J.L., Schmieder, B., Aulanier, G.: 2010, *Space Sci. Rev.* **151**, 333.
Maksimov, V.P., Prokopiev, A.A.: 1995, *Astron. Nachr.* **316**, 249.
Martin, S.F.: 1990, *Lect. Notes Phys.* **363**, 1.
Martin, S.F.: 1998, *Solar Phys.* **182**, 107.
Martin, S.F., Panasenco, O., Berger, M.A., Engvold, O., Lin, Y., Pevtsov, A.A., Srivastava, N.: 2012, In: *Second ATST-EAST Meeting: Magnetic Fields from the Photosphere to the Corona ASP* **CS-463**, 157.
Nagabhushana, B.S., Gokhale, M.H.: 1990, *Lect. Notes Phys.* **363**, 234.
Qu, M., Shih, F.Y., Jing, J., Wang, H.: 2005, *Solar Phys.* **228**, 119.
Scholl, I.F., Habbal, S.R.: 2008, *Solar Phys.* **248**, 425.
Shih, F.Y., Kowalski, A.J.: 2003, *Solar Phys.* **218**, 99.
Tang, F.: 1987, *Solar Phys.* **107**, 233.